

Inferring the effective start dates of non-pharmaceutical interventions during COVID-19 outbreaks

Ilia Kohanovski¹, Uri Obolski^{2,3}, and Yoav Ram^{1,a}

¹School of Computer Science, Interdisciplinary Center Herzliya, Herzliya 4610101, Israel

²School of Public Health, Tel Aviv University, Tel Aviv 6997801, Israel

³Porter School of the Environment and Earth Sciences, Tel Aviv University, Tel Aviv 6997801, Israel

^aCorresponding author: yoav@yoavram.com

July 8, 2020

Abstract

During Feb-Apr 2020, many countries implemented non-pharmaceutical interventions, such as school closures and lockdowns, with variable schedules, to control the COVID-19 pandemic caused by the SARS-CoV-2 virus. Overall, these interventions seem to have successfully reduced the spread of the pandemic. We hypothesise that the official and effective start date of such interventions can significantly differ, for example due to slow adoption by the population, or because the authorities and the public are unprepared. We fit an SEIR model to case data from 12 countries to infer the effective start dates of interventions and contrast them with the official dates. We find mostly late, but also early effects of interventions. For example, Italy implemented a nationwide lockdown on Mar 11, but we infer the effective date on Mar 17 (± 2.99 days 95% CI). In contrast, Germany announced a lockdown on Mar 22, but we infer an effective start date on Mar 19 (± 1.05 days 95% CI). We discuss potential causes and consequences of our results.

Introduction

The COVID-19 pandemic has resulted in implementation of extreme non-pharmaceutical interventions (NPIs) in many affected countries. These interventions, from social distancing to lockdowns, are applied in a rapid and widespread fashion. NPIs are designed and assessed using epidemiological models, which follow the dynamics of infection to forecast the effect of different mitigation and suppression strategies on the levels of infection, hospitalization, and fatality. These epidemiological models usually assume that the effect of NPIs on infection dynamics begins at the officially declared date^{7,9,14}.

Adoption of public-health recommendations is often critical for effective response to infectious diseases, and has been studied in the context of HIV¹³ and vaccination^{4,19}, for example. However, behavioural and social change does not occur immediately, but rather requires time to diffuse in the population through media, social networks, and social interactions. Moreover, compliance to NPIs may differ between different interventions and between people with different backgrounds. For example, in a survey of 2,108 adults in the UK during Mar 2020, Atchison et al.² found that those over 70 years old were more likely to adopt social distancing than young adults (18-34 years old), and that those with lower income were less likely to be able to work from home and to self-isolate. Similarly, compliance to NPIs may be impacted by personal experiences. Smith et al.¹⁶ have surveyed 6,149 UK adults in late Apr 2020 and found that people who believe they have already had COVID-19 are more likely to think they are immune, and less likely to comply with social distancing guidelines. Compliance may also depend on risk perception as perceived by the the number of domestic cases or even by reported cases in other regions and countries. Interestingly, the perceived risk of COVID-19 infection has likely caused a reduction in the number of influenza-like illness cases in the US starting from mid-Feb 2020²⁰.

Here, we hypothesise that there is a significant difference between the official start of NPIs and their effective adoption by the public and therefore their effect on infection dynamics. We use a *Susceptible-Exposed-Infected-Recovered* (SEIR) epidemiological model and a *Markov Chain Monte Carlo* (MCMC) parameter estimation framework to infer the effective start date of NPIs from publicly available COVID-19 case data in 12 geographical regions. We compare these estimates to the

Country	First	Last
Austria	Mar 10 2020	Mar 16 2020
Belgium	Mar 12 2020	Mar 18 2020
Denmark	Mar 12 2020	Mar 18 2020
France	Mar 13 2020	Mar 17 2020
Germany	Mar 12 2020	Mar 22 2020
Italy	Mar 5 2020	Mar 11 2020
Norway	Mar 12 2020	Mar 24 2020
Spain	Mar 9 2020	Mar 14 2020
Sweden	Mar 12 2020	Mar 18 2020
Switzerland	Mar 13 2020	Mar 20 2020
United Kingdom	Mar 16 2020	Mar 24 2020
Wuhan	Jan 23 2020	Jan 23 2020

Table 1: Official start of non-pharmaceutical interventions. The date of the first intervention is for a ban of public events, or encouragement of social distancing, or for school closures. In all countries except Sweden, the date of the last intervention is for a lockdown. In Sweden, where a lockdown was not ordered during the studied dates, the last date is for school closures. Dates for European countries from Flaxman et al.⁷, date for Wuhan, China from Pei and Shaman¹⁵. See Figure S1 for a visual presentation.

official dates, and find that they include both late and early effects of NPIs on infection dynamics. We conclude by demonstrating how differences between the official and effective start of NPIs can confound assessments of the effectiveness of the NPIs in a simple epidemic control framework.

Results

Several studies have described the effects of non-pharmaceutical interventions in different geographical regions^{7,9,14}. Some of these studies have assumed that the parameters of the epidemiological model change at a specific date (Eq. 6), and set the change date τ to the official NPI date τ^* (Table 1). They then fit the model once for time $t < \tau^*$ and once for time $t \geq \tau^*$. For example, Li et al.¹⁴ estimate the infection dynamics in China before and after τ^* , which is set at Jan 23, 2020. Thereby, they effectively estimate the transmission and reporting rates before and after τ^* separately.

Here, we estimate the joint posterior distribution of the *effective* start date of the NPIs τ and the transmission and reporting rates before and after τ from the entire data, rather than splitting the data at τ . We then estimate the marginal posterior probability of τ by marginalising the joint posterior, and estimate $\hat{\tau}$ as the posterior median.

We compare the posterior predictive plots of a model with a free τ with those of a model with τ fixed at τ^* and a model without τ (i.e. transmission and reporting rates are constant). All three models

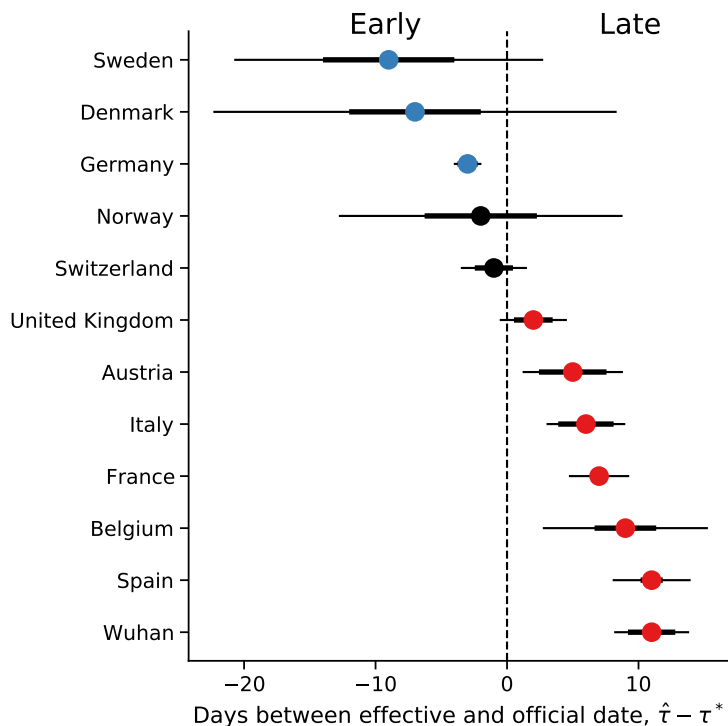


Figure 1: Official vs. effective start of non-pharmaceutical interventions. The difference between $\hat{\tau}$ the effective and τ^* the official start of NPIs is shown for different regions. The effective date is delayed in UK, Austria, Italy, France, Belgium, Spain, and Wuhan, China, compared to the official date (red markers). In contrast, the effective dates in Sweden, Denmark, and Germany are earlier than the official dates (blue markers), although this is significant only for Germany (i.e., zero is not included in 75% CI). The confidence intervals for Sweden, Denmark, and Norway are especially wide, see text and Figure 3 for possible explanation. Here, $\hat{\tau}$ is the posterior median, see Table 2. τ^* is the last NPI date (Table 1). Thin and bold lines show 95% and 75% credible intervals, respectively (i.e. interval in which $P(|\tau - \hat{\tau}| > x | \mathbf{X}) = 0.05$ and 0.25). Figure S2 shows a similar summary when estimating $\hat{\tau}$ using case data up to Mar 28, 2020, rather than Apr 11.

were fitted to case data up to Apr 11, used to predict out-of-sample case data up to Apr 23, and these predictions were then compared to the real case data. The model with free τ clearly produces better and less variable predictions (Figure S4a): In all 11 of the European countries, the expected posterior RMSE (root mean squared error) of the out-of-sample predictions is lowest for the model with a free τ (Table S2). When we compare the models using WAIC (Eq. 9, Table S1), the model with a free τ is strongly preferred in 9 out of 12 countries, the exceptions being Norway (only slight preference), Sweden, and Denmark. Notably, the data for Sweden and Denmark does not have a peak during the evaluated dates, possibly leading to wide 95% confidence intervals on $\hat{\tau}$ (Figure 1) and poor WAIC in the model with free τ , whereas the duration between the first and last interventions was especially long in Norway (Table 1).

We compare the official τ^* and effective $\hat{\tau}$ start of NPIs and find that in most regions (10 of 12) the effective start of NPIs significantly differs from the official date (Figure 1), that is, the 75% credible interval on $\hat{\tau}$ does not include τ^* (Figure 1). The exceptions are Switzerland (see below), and Norway. The latter also has a wide 95% credible interval, perhaps because it has the longest duration between the first and last NPIs (Table 1). In the following, we describe our findings in more detail.

Late effective start of NPIs. In half of the examined regions, we estimate that the effective start of NPIs $\hat{\tau}$ is significantly later than the official date τ^* .

In Italy, the first case was officially confirmed on Feb 21. School closures were implemented on Mar 5⁷, a lockdown was declared in Northern Italy on Mar 8, with social distancing implemented in the rest of the country, and the lockdown was extended to the entire nation on Mar 11⁹. That is, the first and last official NPI dates are Mar 8 and Mar 11. However, we estimate the effective date $\hat{\tau}$ at Mar 17 (± 2.99 days 95% CI ; Figure 2).

In Wuhan, China, a lockdown was ordered on Jan 23¹⁴, but we estimate the effective start of NPIs to be more than a week later, at Feb 3 (± 2.85 days 95% CI; Figure 2).

In Spain, social distancing was encouraged starting on Mar 8⁷, but mass gatherings still occurred on Mar 8, including a march of 120,000 people for the [International Women's Day](#), and a football match between [Real Betis and Real Madrid](#) (final score: 2–1) with a crowd of 50,965 in Seville. A national lockdown was only announced on Mar 14⁷. Nevertheless, we estimate the effective start of NPI $\hat{\tau}$ on Mar 24 (± 2.96 days 95 %CI), rather than Mar 14 (Figure 2).

Similarly, in France we estimate the effective start of NPIs $\hat{\tau}$ on Mar 24 (± 2.29 days 95% CI, Figure 2). This is about a week later than the official lockdown, which started at Mar 17, and more than 10 days after the earliest NPI, banning of public events, which started on Mar 13⁷.

Interestingly, the effect of NPIs $\hat{\tau}$ in both France and Spain is estimated to have started on Mar 24, although the official NPI dates differ significantly: the first NPI in France is only one day before the last NPI in Spain. The number of daily cases was similar in both countries until Mar 8, but diverged by Mar 13, reaching significantly higher numbers in Spain (Figure S3). This may suggest correlations between effective starts of NPIs due to global or international events.

Early effective start of NPIs. In some regions we estimate an effective start of NPIs $\hat{\tau}$ that is *earlier* than the official date τ^* (Figure 1). The only significant early case is Germany, in which we estimate the effective start of NPIs at Mar 19 (± 1.05 days 95 %CI; Figure 3). This estimate falls between the first and last official NPI dates, Mar 12 and Mar 22 (Table 1). Therefore, when we refer to this case as "early", we mean that the effective date (Mar 19) occurs *before* the official lockdown date (Mar 22), not that it occurs before all the NPIs. Interestingly, Germany has the second longest duration between first and last NPIs after Norway (10 and 12 days respectively; see Table 1). Nevertheless, the credible

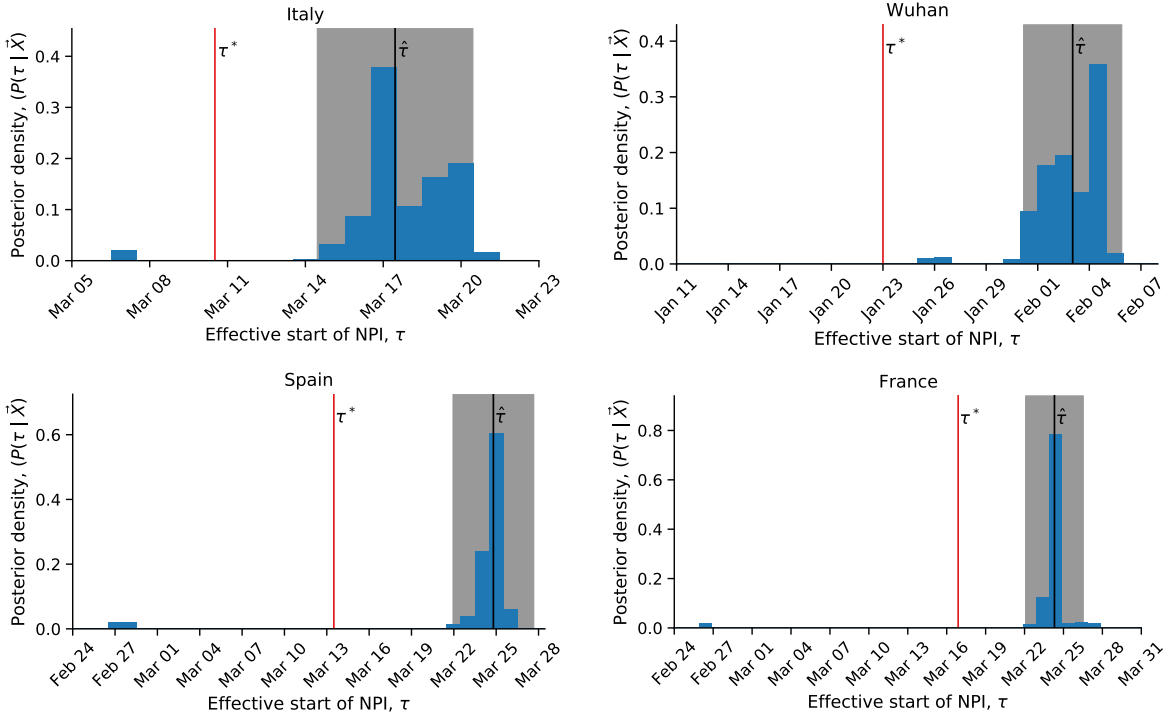


Figure 2: Late effect of non-pharmaceutical interventions. Posterior distribution of τ , the effective start date of NPI, is shown as a histogram of MCMC samples. Red line shows the official last NPI date τ^* . Black line shows the estimate $\hat{\tau}$. Shaded area shows a 95% credible interval (interval in which $P(|\tau - \hat{\tau}| | \bar{X}) = 0.95$).

interval for the effective date in Germany is narrow (± 1.05 days 95 %CI), whereas it is quite wide in Norway (± 10.79 days; Figure 3).

We also estimate early effective start of NPIs in Sweden and Denmark. However, the credible intervals are quite wide (Figure 1), and the fit of the model with free τ wasn't significantly better than the fit of the model with τ fixed at the official date (Table S2, Table S1). In Sweden, the data does not "peak", i.e., the number of daily cases continues to grow up to Apr 11 (Figure S4a). In Denmark, the opposite occurs: there are seemingly two "peaks", on Mar 11 and on Apr 8 (Figure S4a); the first "peak" may be a result of stochastic events, for example due to a large cluster of cases or an accumulation of tests. We suspect that these missing and additional "peaks" increase the uncertainty in our inference.

Early effective start of NPIs. We find one case in which the official and effective dates match "*like a Swiss watch*", and the credible interval is narrow: Switzerland ordered a national lockdown on Mar 20, after banning public events and closing schools on Mar 13 and 14⁷. Indeed, the posterior median $\hat{\tau}$ is Mar 19 (± 2.51 days 95% CI, see Figure 3). It's also worth mentioning that Switzerland was the first to mandate self isolation of confirmed cases⁷.

The estimated effective date in Norway is Mar 22 (± 10.79 days 95% CI), which doesn't significantly differ from the official date of Mar 24. However, the posterior distribution is very wide (Figure 3): it covers the range between Mar 9, three days before the first NPI, and Mar 29, five days after the last NPI (see Table 1 and Figure S1 for NPI dates). The uncertainty in the estimate of the effective start of NPIs may be due to the long duration between the first and last NPI; however, Germany had the second longest duration between first and last NPIs, but the corresponding posterior distribution is quite narrow (Figure 3).

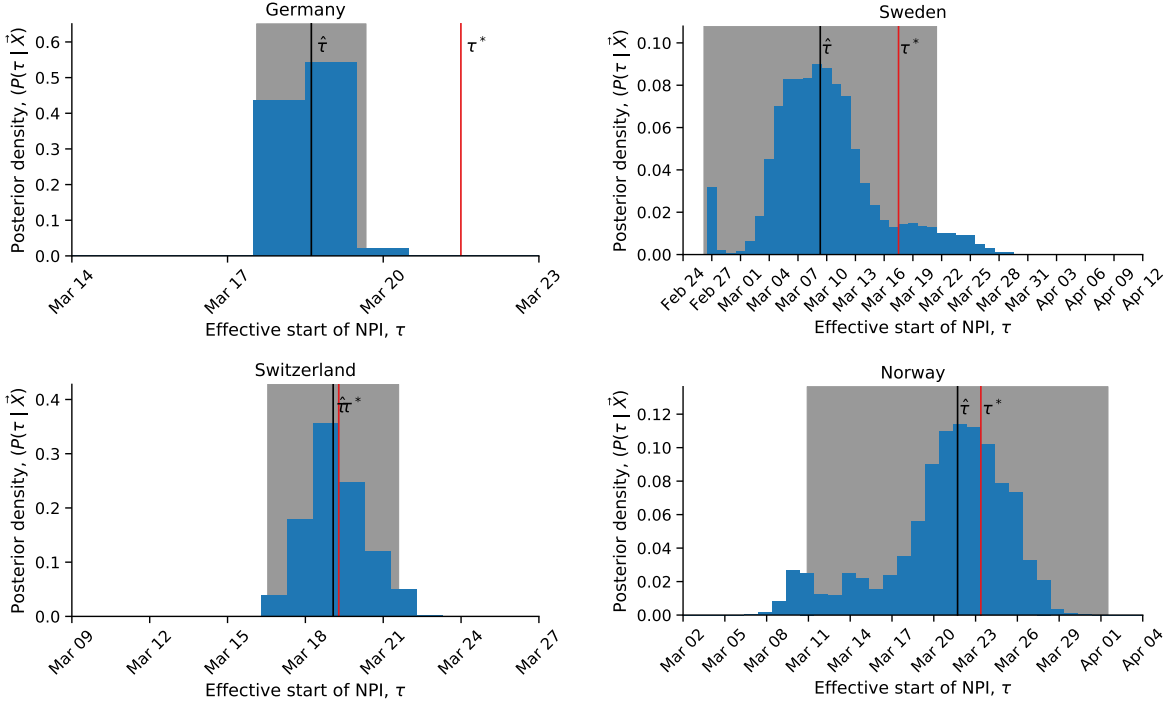


Figure 3: Early and exact effect of non-pharmaceutical interventions. Posterior distribution of τ , the effective start date of NPI, is shown as a histogram of MCMC samples. Red line shows the official last NPI date τ^* . Black line shows the estimated $\hat{\tau}$. Shaded area shows a 95% credible interval (interval in which $P(|\tau - \hat{\tau}| | \bar{X}) = 0.95$).

Consequences of late and early effect of NPIs on real-time assessment. The success of non-pharmaceutical interventions is assessed by health officials using various metrics, such as the decline in the growth rate of daily cases. These assessments are made a specific number of days after the intervention began, to accommodate for the expected serial interval³ (i.e. time between successive cases in a chain of transmission), which is estimated at about 4-7 days⁹.

However, a significant difference between the beginning of the intervention and the effective change in transmission rates can invalidate assessments that assume a serial interval of 4-7 days and neglect the late or early population response to the NPI. This is illustrated in Figure 4 using data and parameters from Italy: a lockdown was officially ordered on Mar 10 (τ^*), but its late effect on the infection dynamics starts on Mar 17 ($\hat{\tau}$). If health officials assumed the dynamics to immediately change at τ^* , they will have expected the number of cases to be within the red lines (posterior predictions assuming $\tau = \tau^*$). This would have led to a significant underestimation, which might have been interpreted by as ineffectiveness of the NPI, leading to further escalations. However, the number of cases would actually follow the blue lines (posterior predictions using $\tau = \hat{\tau}$), which corresponds well to the real data (stars).

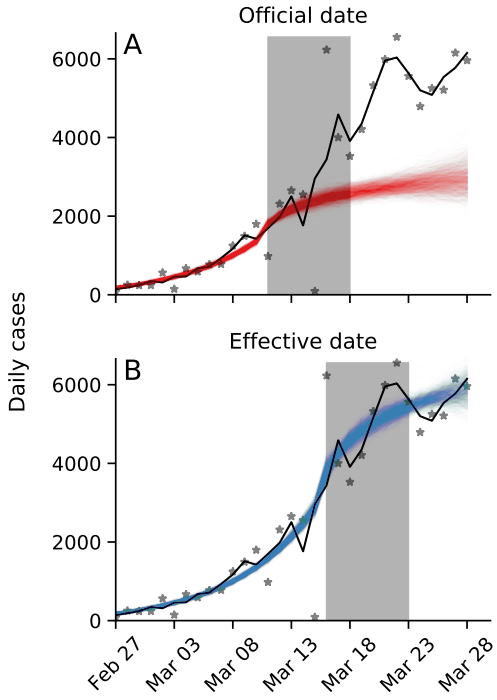


Figure 4: Late effective start of NPIs leads to underestimation of daily confirmed cases. Real number of daily cases in Italy in black (markers: data, line: time moving average). Model posterior predictions are shown as coloured lines (1,000 draws from the posterior distribution). Shaded box illustrates a serial interval of seven days. **(A)** Using the official date τ^* for the start of the NPI, the model underestimates the number of cases seven days after the start of the NPI. **(B)** Using the effective date $\hat{\tau}$ for the start of the NPI, the model correctly estimates the number of cases seven days after the start of the NPI. Here, model parameters are best estimates for Italy (Table 2).

Discussion

We have inferred the effective start date of NPIs in several geographical regions using an SEIR epidemiological model and an MCMC parameter estimation framework. We find examples of both late and early effect of NPIs (Figure 1).

In most investigated countries we find a late effect of NPI on the transmission dynamics. For example, in Italy and in Wuhan, China, the effective start of the lockdowns seems to have occurred five days or more after the official date (Figure 2). This difference might be explained, in some case, by low compliance: In Italy, for example, the government intention to lockdown Northern provinces leaked to the public, resulting in people leaving those provinces⁹. Late effect of NPIs may also be due to the time required by both the government and the citizens to organise for a lockdown, and for the new guidelines to be adopted by the population.

In contrast, in some regions we inferred reduced transmission rates even before official lockdowns were implemented (Figure 3), although this is only significant for Germany (Figure 1). An early effective date might be due to early adoption of social distancing and similar behavioural adaptations in parts of the population. Adoption of these behaviours may occur via media and social networks, rather than official government recommendations and instructions, and may be influenced by increased risk perception due to domestic or international COVID-19-related reports¹. Indeed, the evidence supports a change in infection dynamics (i.e. a model with fixed or free τ) even for Sweden (Table S2, Table S1, Figure S4a), where a lockdown was not implemented*.

*Sweden banned public events on Mar 12, encouraged social distancing on Mar 16, and closed schools on Mar 18⁷.

Attempts to assess the effect of NPIs^{3,7} generally assume a seven-day delay between the implementation of the intervention and the observable change in dynamics, due to the characteristic serial interval of COVID-19⁹. However, late and early effects such as we have inferred may bias these assessments and lead to wrong conclusions about the effects of NPIs (Figure 4).

We have found that the evidence supports a model in which the parameters change at a specific time point τ over a model without such a change-point in most regions (i.e. free or fixed model in Table S2 and Table S1). It may be interesting to check if the evidence favors a model with *two* change-points, rather than one. Two such change-points could reflect escalating NPIs (e.g. school closures followed by lockdowns), or an intervention followed by a relaxation. However, interpretation of such models will be harder, as two change-points can also reflect a mix of NPIs and other events, such as changing weather, news of new treatments, and international outbreaks.

As different countries experiment with various interventions strategies, we expect similar delays and advances to occur: in some cases the population will be late to comply with guidelines, whereas in other cases the population will adopt restrictions or relaxations even before they are formally declared.

Conclusions. We have inferred the effective start date of NPIs and found that they often differ from the official dates. Our results highlight the complex interaction between personal, regional, and global determinants of behavioral response to an epidemic. Therefore, we emphasize the need to further study variability in compliance and behavior over both time and space. This can be accomplished both by surveying differences in compliance within and between populations², and by incorporating specific behavioral models into epidemiological models^{1,5,18}.

Models and Methods

Data. We use daily confirmed case data $\mathbf{X} = (X_1, \dots, X_T)$ from 12 regions during Jan–Apr 2020. These incidence data summarise the number of individuals X_t tested positive for SARS-CoV-2 RNA (using RT-qPCR) at each day t . Data for Wuhan, China retrieved from Pei and Shaman¹⁵, data for 11 European countries retrieved from Flaxman et al.⁷. Where there were multiple sequences of days with zero confirmed cases (e.g. France), we cropped the data to begin with the last sequence so that our analysis focuses on the first sustained outbreak rather than isolated imported cases. For official NPI dates see Table 1.

SEIR model. We model SARS-CoV-2 infection dynamics by following the number of susceptible S , exposed E , reported infected I_r , unreported infected I_u , and recovered R individuals in a population of size N . This model distinguishes between reported and unreported infected individuals: the reported infected are those that have enough symptoms to eventually be tested and thus appear in daily case reports, to which we fit the model. This model is inspired by Li et al.¹⁴ and Pei and Shaman¹⁵, who used a similar model with multiple regions and constant transmission and reporting rates to study COVID-19 dynamics in China and in the continental US.

Susceptible (S) individuals become exposed due to contact with reported or unreported infected individuals (I_r or I_u) at a rate β_t or $\mu\beta_t$, respectively. The parameter $0 < \mu < 1$ represents the decreased transmission rate from unreported infected individuals, who are often subclinical or even asymptomatic^{6,17}. The transmission rate $\beta_t \geq 0$ may change over time t due to behavioural changes of both susceptible and infected individuals. Exposed individuals, after an average incubation period of Z days, become reported infected with probability α_t or unreported infected with probability $(1 - \alpha_t)$. The reporting rate $0 < \alpha_t < 1$ may also change over time due to changes in human behaviour. Infected individuals remain infectious for an average period of D days, after which they either recover, or become ill enough to be quarantined. In either case, they no longer infect

other individuals, and therefore effectively become recovered (R). The model is described by the following set of equations:

$$\begin{aligned}\frac{dS}{dt} &= -\beta_t S \frac{I_r}{N} - \mu \beta_t S \frac{I_u}{N} \\ \frac{dE}{dt} &= \beta_t S \frac{I_r}{N} + \mu \beta_t S \frac{I_u}{N} - \frac{E}{Z} \\ \frac{dI_r}{dt} &= \alpha_t \frac{E}{Z} - \frac{I_r}{D} \\ \frac{dI_u}{dt} &= (1 - \alpha_t) \frac{E}{Z} - \frac{I_r}{D} \\ \frac{dR}{dt} &= \frac{I_r}{D} + \frac{I_r}{D}.\end{aligned}\tag{1}$$

The initial numbers of exposed $E(0)$ and unreported infected $I_u(0)$ are free model parameters (i.e. inferred from the data), whereas the initial number of reported infected and recovered is assumed to be zero, $I_r(0) = R(0) = 0$, and the number of susceptible is $S(0) = N - E(0) - I_u(0)$.

Likelihood function. For a given vector θ of model parameters the *expected* cumulative number of reported infected individuals (I_r) until day t , following Eq. 1, is

$$Y_t(\theta) = \int_0^t \alpha_s \frac{E(s)}{Z} ds, \quad Y_0 = 0.\tag{2}$$

We assume that reported infected individuals are confirmed and therefore observed in the daily case report of day t with probability p_t (note that an individual can only be observed once, and that p_t may change over time, but t is a specific date rather than the time elapsed since the individual was infected). We denote by X_t the *observed* number of confirmed cases in day t , and by \tilde{X}_t the cumulative number of confirmed cases until end of day t ,

$$\tilde{X}_t = \sum_{i=1}^t X_i.\tag{3}$$

Therefore, at day t the number of reported infected yet-to-be confirmed individuals is $(Y_t(\theta) - \tilde{X}_{t-1})$. We therefore assume that X_t conditioned on \tilde{X}_{t-1} is Poisson distributed, such that

$$\begin{aligned}(X_1 | \theta) &\sim Poi(Y_1(\theta) \cdot p_1), \\ (X_t | \tilde{X}_{t-1}, \theta) &\sim Poi((Y_t(\theta) - \tilde{X}_{t-1}) \cdot p_t), \quad t = 2, \dots, T.\end{aligned}\tag{4}$$

Hence, the *likelihood function* $\mathcal{L}(\theta | \mathbf{X})$ for a parameter vector θ given the confirmed case data $\mathbf{X} = (X_1, \dots, X_T)$ is defined by the probability to observe \mathbf{X} given θ ,

$$\mathcal{L}(\theta | \mathbf{X}) = P(\mathbf{X} | \theta) = P(X_1 | \theta) \cdot P(X_2 | \tilde{X}_1, \theta) \cdots P(X_T | \tilde{X}_{T-1}, \theta).\tag{5}$$

NPI model. To model non-pharmaceutical interventions (NPIs), we set the start of the NPIs to day τ and define

$$\beta_t = \begin{cases} \beta, & t < \tau \\ \beta\lambda, & t \geq \tau \end{cases}, \quad \alpha_t = \begin{cases} \alpha_1, & t < \tau \\ \alpha_2, & t \geq \tau \end{cases}, \quad p_t = \begin{cases} 1/9, & t < \tau \\ 1/6, & t \geq \tau \end{cases},\tag{6}$$

where $0 < \lambda < 1$. The values for p_t follow Li et al.¹⁴, who estimated the average time between infection and reporting in Wuhan, China, at 9 days before the start of NPIs and 6 days after start of NPIs.

Parameter estimation. To estimate the model parameters from the daily case data \mathbf{X} , we apply a Bayesian inference approach. We start our model Δt days⁹ before the outbreak (defined as consecutive days with increasing confirmed cases) in each country. The model in Eq. 1 is parameterised by the vector θ , where

$$\theta = \left(Z, D, \mu, \{\beta_t\}, \{\alpha_t\}, \{p_t\}, E(0), I_u(0), \tau, \Delta t \right). \quad (7)$$

The likelihood function is defined in Eq. 5. The posterior distribution of the model parameters $P(\theta | \mathbf{X})$ is estimated using the affine-invariant ensemble sampler for Markov chain Monte Carlo (MCMC)¹¹ implemented in the emcee Python package⁸.

We defined the following prior distributions on the model parameters $P(\theta)$:

$$\begin{aligned} Z &\sim Uniform(2, 5) \\ D &\sim Uniform(2, 5) \\ \mu &\sim Uniform(0.2, 1) \\ \beta &\sim Uniform(0.8, 1.5) \\ \lambda &\sim Uniform(0, 1) \\ \alpha_1, \alpha_2 &\sim Uniform(0.02, 1) \\ E(0) &\sim Uniform(0, 3000) \\ I_u(0) &\sim Uniform(0, 3000) \\ \Delta t &\sim Uniform(1, 5) \\ \tau &\sim TruncatedNormal\left(\frac{\tau^* + \tau^0}{2}, \frac{\tau^* - \tau^0}{2}, 1, T - 2\right), \end{aligned} \quad (8)$$

where the prior for τ is a truncated normal distribution shaped so that the date of the first and last NPI, τ^0 and τ^* (Table 1), are at minus and plus one standard deviation, and taking values only between 1 and $T - 2$, where T is the number of days in the data \mathbf{X} . We also tested an uninformative uniform prior, $Uniform(1, T - 2)$. WAIC (Eq. 9) of a model with this uniform prior was either higher, or lower by less than 2, compared to WAIC of a model with the truncated normal prior. The uninformative prior resulted in non-negligible posterior probability for unreasonable τ values, such as Mar 1 in the United Kingdom. This was probably due to MCMC chains being stuck in low posterior regions of the parameter space. We therefore decided to use the more informative truncated normal prior for τ . Other priors follow Li et al.¹⁴, with the following exceptions. λ is used to ensure transmission rates are lower after the start of the NPIs ($\lambda < 1$). We checked values of Δt larger than five days and found they generally produce lower likelihood and unreasonable parameter estimates, and therefore chose $Uniform(1, 5)$ as the prior for Δt . Model fitting was calibrated for case data up to Mar 28, and then applied to data up to Apr 11.

Model comparison. We perform model selection using two methods. First, we compute WAIC (widely applicable information criterion)¹⁰,

$$WAIC(\theta, \mathbf{X}) = -2 \log \mathbb{E}[\mathcal{L}(\theta | \mathbf{X})] + 2\mathbb{V}[\log \mathcal{L}(\theta | \mathbf{X})] \quad (9)$$

where $\mathbb{E}[\cdot]$ and $\mathbb{V}[\cdot]$ are the expectation and variance operators taken over the posterior distribution $P(\theta | \mathbf{X})$. We compare models by reporting their relative WAIC; lower is better (Table S1). A minority (<5%) of MCMC chains that fail to fully converge can lead to overestimation of the variance (the second term in Eq. 9). Therefore, we exclude from the computation of WAIC chains with mean log-likelihood that is three standard deviations or more from the overall mean.

We also plot posterior predictions: we sample 1,000 parameter vectors from the posterior distribution $P(\theta | \mathbf{X})$ fitted to data up to Apr 11, use these parameter vectors to simulate the SEIR model (Eq. 1) from Apr 12 to Apr 24, and plot the predicted dynamics (Figure S4a). Both the accuracy (i.e. overlap of data and prediction) and the precision (i.e. the tightness of the predictions) are good ways to visually compare models. We also compute the expected posterior root mean squared error of these predictions (Table S2).

Source code. We use Python 3 with the NumPy, Matplotlib, SciPy, Pandas, Seaborn, and emcee packages. All source code will be publicly available under a permissive open-source license at github.com/yoavram-lab/EffectiveNPI. Samples from the posterior distributions will be deposited on FigShare.

Country	τ^*	τ	$CI_{75\%}$	$CI_{95\%}$	Z	D	μ	β	α_1	λ	α_2	$E(0)$	$I_u(0)$	Δt
Austria	Mar 16	Mar 21	2.5658	3.8148	3.9102	3.6649	0.6407	1.1417	0.1308	0.1387	0.2261	151.1078	131.6623	2.1308
Belgium	Mar 18	Mar 27	2.3456	6.2773	3.9098	3.6152	0.4877	1.0762	0.2721	0.4388	0.2363	309.9114	426.9644	2.1756
Denmark	Mar 18	Mar 11	5.0053	15.3374	4.0957	3.5091	0.4161	1.0747	0.1470	0.6919	0.1867	324.6332	389.5076	2.2071
France	Mar 17	Mar 24	0.5068	2.2928	4.2159	3.1688	0.4863	1.0502	0.3726	0.3765	0.4168	422.6720	1362.5052	1.6717
Germany	Mar 22	Mar 19	0.7657	1.0508	3.3917	3.7166	0.6780	1.1515	0.1753	0.2664	0.4147	529.9397	387.1038	2.1516
Italy	Mar 11	Mar 17	2.1045	2.9945	4.1439	2.5550	0.5371	0.9932	0.5816	0.3860	0.4973	990.1942	1902.7806	1.6367
Norway	Mar 24	Mar 22	4.2700	10.7889	4.0476	3.1061	0.3885	1.0467	0.1536	0.3091	0.2320	478.0678	856.7700	1.9998
Spain	Mar 14	Mar 25	0.8415	2.9656	4.1392	3.3352	0.5974	1.1574	0.3640	0.2551	0.3050	310.0470	957.8280	1.6062
Sweden	Mar 18	Mar 09	4.9930	11.7493	4.0328	3.3962	0.3656	1.0457	0.1427	0.7237	0.3093	394.0202	543.5448	2.3755
Switzerland	Mar 20	Mar 19	1.4513	2.5140	3.9764	3.4425	0.6360	1.1543	0.1283	0.2481	0.2246	336.3842	328.7800	1.9891
United Kingdom	Mar 24	Mar 26	1.4721	2.5543	3.9654	3.6333	0.6414	1.1168	0.1212	0.4504	0.1737	422.8841	486.0467	2.0540
Wuhan, China	Jan 23	Feb 03	1.7984	2.8493	3.7326	3.6320	0.6057	1.1453	0.2754	0.1784	0.3511	597.8676	561.1586	2.4248

Table 2: Parameter estimates for different regions. See Eq. 1 for model parameters. All estimates are posterior medians. 75% and 95% credible intervals given for τ , in days. τ^* is the official last NPI date, see Table 1.

Acknowledgements

We thank Lilach Hadany and Oren Kolodny for discussions and comments. This work was supported in part by the Israel Science Foundation 3811/19 and 1399/17.

References

- [1] Arthur, R. F., Jones, J. H., Bonds, M. H. and Feldman, M. W. 2020, ‘Complex dynamics induced by delayed adaptive behavior during outbreaks’, *bioRxiv* pp. 1–23.
- [2] Atchison, C. J., Bowman, L., Vrinten, C., Redd, R., Pristera, P., Eaton, J. W. and Ward, H. 2020, ‘Perceptions and behavioural responses of the general public during the COVID-19 pandemic: A cross-sectional survey of UK Adults’, *medRxiv* p. 2020.04.01.20050039.
- [3] Banholzer, N., Weenen, E. V., Kratzwald, B. and Seeliger, A. 2020, ‘The estimated impact of non-pharmaceutical interventions on documented cases of COVID-19 : A cross-country analysis’, *medRxiv*.
- [4] Dunn, A. G., Leask, J., Zhou, X., Mandl, K. D. and Coiera, E. 2015, ‘Associations between exposure to and expression of negative opinions about human papillomavirus vaccines on social media: An observational study’, *J. Med. Internet Res.* **17**(6), e144.
- [5] Fenichel, E. P., Castillo-Chavez, C., Ceddia, M. G., Chowell, G., Gonzalez Parrae, P. A., Hickling, G. J., Holloway, G., Horan, R., Morin, B., Perrings, C., Springborn, M., Velazquez, L. and Villalobos, C. 2011, ‘Adaptive human behavior in epidemiological models’, *Proc. Natl. Acad. Sci. U. S. A.* **108**(15), 6306–6311.
- [6] Ferretti, L., Wymant, C., Kendall, M., Zhao, L., Nurtay, A., Abeler-Dörner, L., Parker, M., Bonsall, D. and Fraser, C. 2020, ‘Quantifying SARS-CoV-2 transmission suggests epidemic control with digital contact tracing’, *Science (80-.).* **368**(6491), eabb6936.
- [7] Flaxman, S., Mishra, S., Gandy, A., Unwin, J. T., Coupland, H., Mellan, T. A., Zhu, H., Berah, T., Eaton, J. W., Guzman, P. N. P., Schmit, N., Cilloni, L., Ainslie, K. E. C., Baguelin, M., Blake, I., Boonyasiri, A., Boyd, O., Cattarino, L., Ciavarella, C., Cooper, L., Cucunubá, Z., Cuomo-Dannenburg, G., Dighe, A., Djaafara, B., Dorigatti, I., Van Elsland, S., Fitzjohn, R., Fu, H., Gaythorpe, K., Geidelberg, L., Grassly, N., Green, W., Hallett, T., Hamlet, A., Hinsley, W., Jeffrey, B., Jorgensen, D., Knock, E., Laydon, D., Nedjati-Gilani, G., Nouvellet, P., Parag, K., Siveroni, I., Thompson, H., Verity, R., Volz, E., Gt Walker, P., Walters, C., Wang, H., Wang, Y., Watson, O., Xi, X., Winskill, P., Whittaker, C., Ghani, A., Donnelly, C. A., Riley, S., Okell, L. C., Vollmer, M. A. C., Ferguson, N. M. and Bhatt, S. 2020, ‘Estimating the number of infections and the impact of non-pharmaceutical interventions on COVID-19 in 11 European countries’, *Imp. Coll. London* (March), 1–35.
- [8] Foreman-Mackey, D., Hogg, D. W., Lang, D. and Goodman, J. 2013, ‘emcee : The MCMC Hammer’, *Publ. Astron. Soc. Pacific* **125**(925), 306–312.
- [9] Gatto, M., Bertuzzo, E., Mari, L., Miccoli, S., Carraro, L., Casagrandi, R. and Rinaldo, A. 2020, ‘Spread and dynamics of the COVID-19 epidemic in Italy: Effects of emergency containment measures’, *Proc. Natl. Acad. Sci.* p. 202004978.
- [10] Gelman, A., Carlin, J. B., Stern, H. S., Dunson, D. B., Vehtari, A. and Rubin, D. B. 2013, *Bayesian Data Analysis, Third Edition*, Chapman & Hall/CRC Texts in Statistical Science, Taylor & Francis.

- [11] Goodman, J. and Weare, J. 2010, ‘Ensemble Samplers With Affine Invariance’, *Commun. Appl. Math. Comput. Sci.* **5**(1), 65–80.
- [12] Kass, R. E. and Raftery, A. E. 1995, ‘Bayes Factors’, *J. Am. Stat. Assoc.* **90**(430), 773.
- [13] Kaufman, M. R., Cornish, F., Zimmerman, R. S. and Johnson, B. T. 2014, ‘Health behavior change models for HIV prevention and AIDS care: Practical recommendations for a multi-level approach’, *J. Acquir. Immune Defic. Syndr.* **66**(SUPPL.3), 250–258.
- [14] Li, R., Pei, S., Chen, B., Song, Y., Zhang, T., Yang, W. and Shaman, J. 2020, ‘Substantial undocumented infection facilitates the rapid dissemination of novel coronavirus (SARS-CoV2)’, *Science* (80-.). p. eabb3221.
- [15] Pei, S. and Shaman, J. 2020, ‘Initial Simulation of SARS-CoV2 Spread and Intervention Effects in the Continental US’, *medRxiv* p. 2020.03.21.20040303.
- [16] Smith, L. E., Mottershaw, A. L., Egan, M., Waller, J., Marteau, T. M. and Rubin, G. J. 2020, ‘The impact of believing you have had COVID-19 on behaviour : Cross-sectional survey’, *medRxiv* pp. 1–20.
- [17] Thompson, R. N., Lovell-Read, F. A. and Obolski, U. 2020, ‘Time from Symptom Onset to Hospitalisation of Coronavirus Disease 2019 (COVID-19) Cases: Implications for the Proportion of Transmissions from Infectors with Few Symptoms’, *J. Clin. Med.* **9**(5), 1297.
- [18] Walters, C. E. and Kendal, J. R. 2013, ‘An SIS model for cultural trait transmission with conformity bias’, *Theor. Popul. Biol.* **90**, 56–63.
- [19] Wiyeh, A. B., Cooper, S., Nnaji, C. A. and Wiysonge, C. S. 2018, ‘Vaccine hesitancy ’outbreaks’: using epidemiological modeling of the spread of ideas to understand the effects of vaccine related events on vaccine hesitancy’, *Expert Rev. Vaccines* **17**(12), 1063–1070.
- [20] Zipfel, C. M. and Bansal, S. 2020, ‘Assessing the interactions between COVID-19 and influenza in the United States’, *medRxiv* (February), 1–13.

Supplementary Material

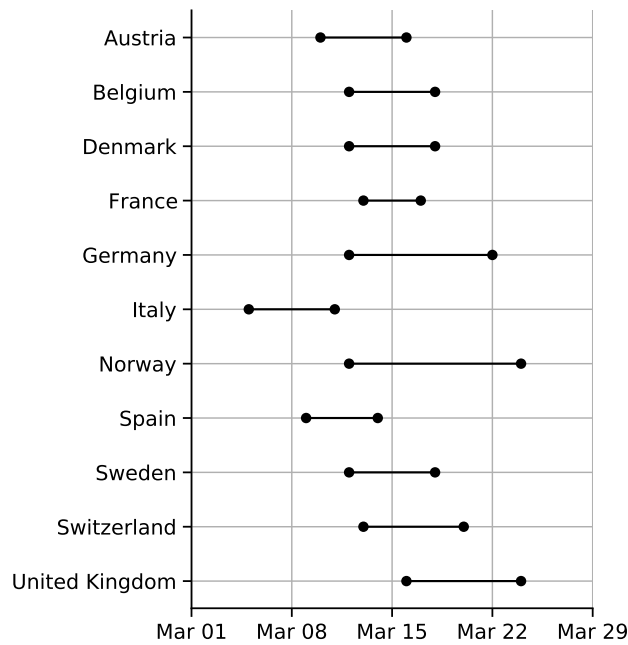


Figure S1: Official start of non-pharmaceutical interventions. See Table 1 for more details. Wuhan, China is not shown.

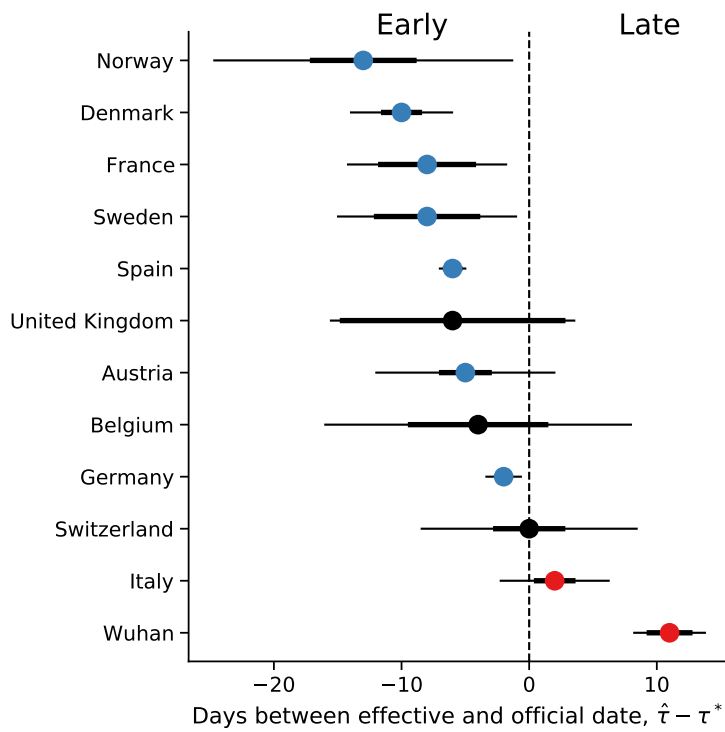


Figure S2: Official vs. effective start of non-pharmaceutical interventions estimated up to Mar 28. The difference between $\hat{\tau}$ the effective and τ^* the official start of NPIs estimated from case data up to Mar 28, 2020, shown for different regions. Here, $\hat{\tau}$ is the posterior median, see Table 2. τ^* is the last NPI date (Table 1). Thin and bold lines show 95% and 75% credible intervals, respectively (i.e. interval in which $P(|\tau - \hat{\tau}| > 1.96 \text{ days} | \mathbf{X}) = 0.05$ and $P(|\tau - \hat{\tau}| > 1.28 \text{ days} | \mathbf{X}) = 0.075$.)

WAIC

Country	No	Fixed	Free
Austria	219.49	95.06	35.96
Belgium	148.37	98.41	49.16
Denmark	44.36	40.30	43.11
France	581.59	255.14	172.08
Germany	1029.36	327.50	174.90
Italy	898452.34	5484.56	80.18
Norway	70.03	42.04	39.79
Spain	1476.46	647.34	128.58
Sweden	32.53	30.06	31.10
Switzerland	265.80	83.95	63.89
United Kingdom	258.18	117.54	68.17
Wuhan China	107.31	94.00	73.75

Table S1: WAIC values for the different models. WAIC (widely applicable information criterion; Eq. 9)¹⁰ values for models with: no τ at all, *No*; τ fixed at the official last NPI date τ^* , *Fixed*; and free parameter τ , *Free*. WAIC values are scaled as a deviance measure: lower values imply higher predictive accuracy and a difference of 2 is a popular significance level for model comparison¹². Bold values emphasize cases in which the *Free* model has the lowest WAIC.

RMSE

Country	No	Fixed	Free
Austria	926.7	740.7	58.9
Belgium	3286.0	2541.0	902.9
Denmark	434.8	1058.0	400.0
France	10530.0	8206.0	1816.0
Germany	14240.0	17760.0	1952.0
Italy	14160.0	9536.0	1106.0
Norway	292.2	578.2	63.3
Spain	17840.0	14410.0	1704.0
Sweden	775.9	1205.0	596.4
Switzerland	1839.0	1721.0	214.0
United Kingdom	14700.0	14780.0	2735.0

Table S2: Posterior RMSE of out-of-sample predictions with the different models. Expected posterior predictive RMSE (root mean squared error) for models with: no τ at all, *No*; τ fixed at the official last NPI date τ^* , *Fixed*; and free parameter τ , *Free*. In all cases, the model with free parameter τ has the lowest RMSE. Models were fitted to case data up to Apr 11, 2020, and then used to generate 1,000 predictions from Apr 12 to Apr 24 by sampling model parameters from the posterior distribution. These predictions were then compared to the real data using RMSE, and the mean RMSE value is shown in the table for each country and model. Bold values emphasize cases in which the *Free* model has the lowest RMSE.

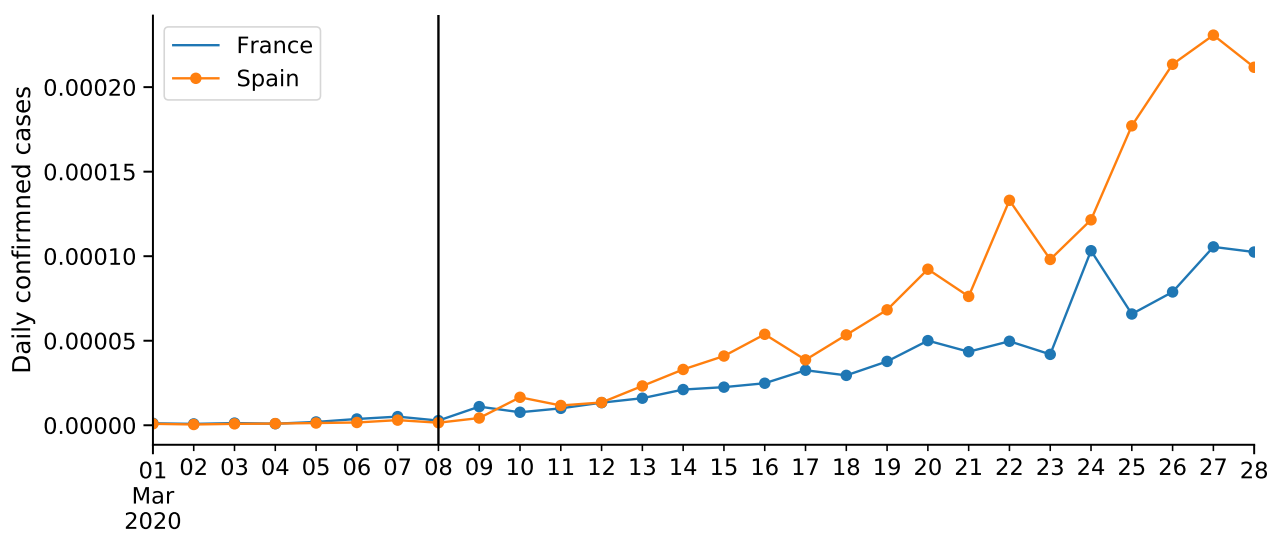
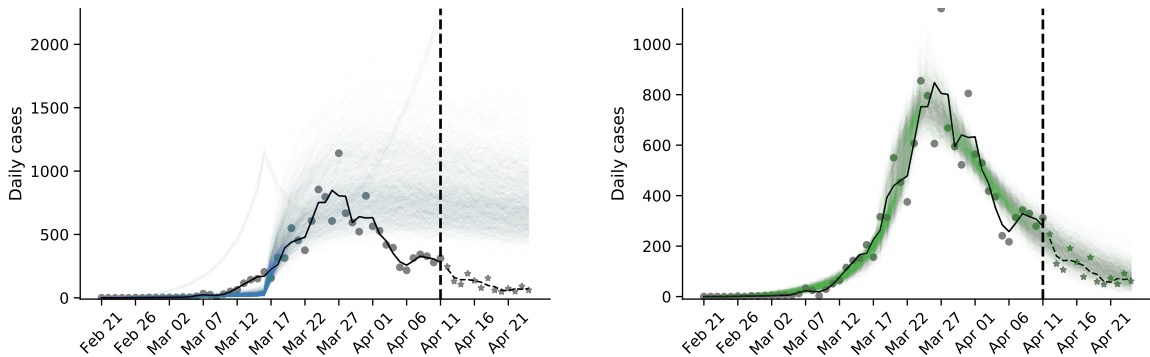
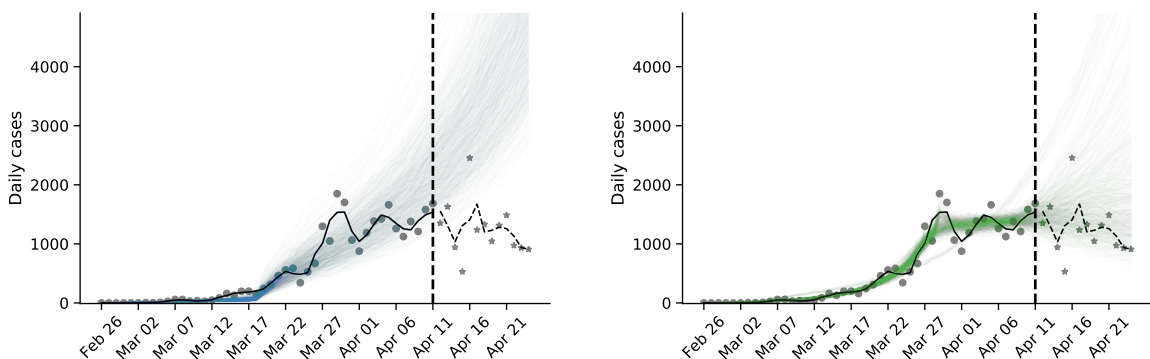


Figure S3: COVID-19 confirmed cases in France and Spain. Number of cases proportional to population size (as of 2018). Vertical line shows Mar 8, the effective start of NPIs $\hat{\tau}$ in both countries.

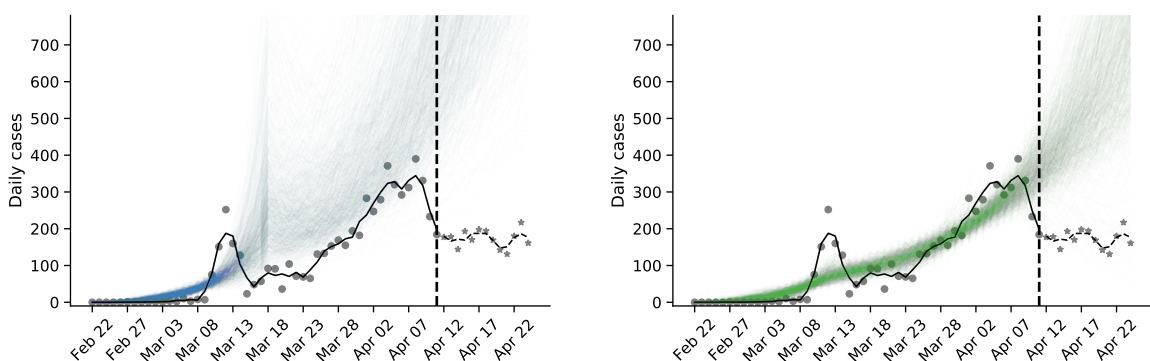
Austria



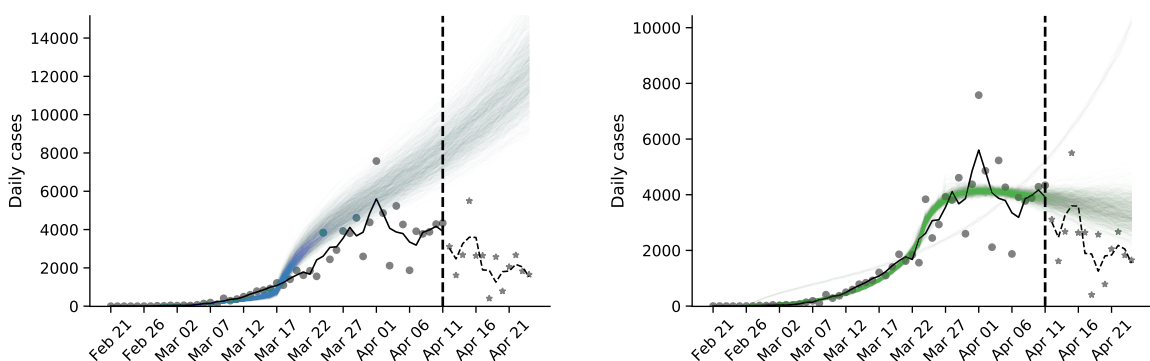
Belgium



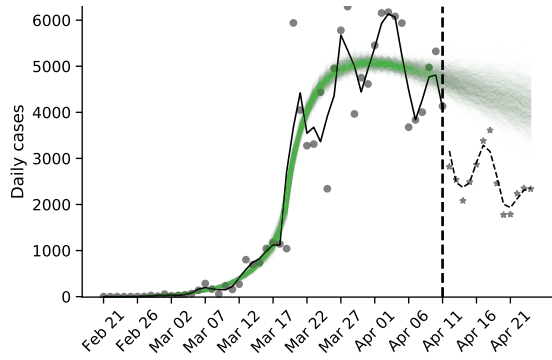
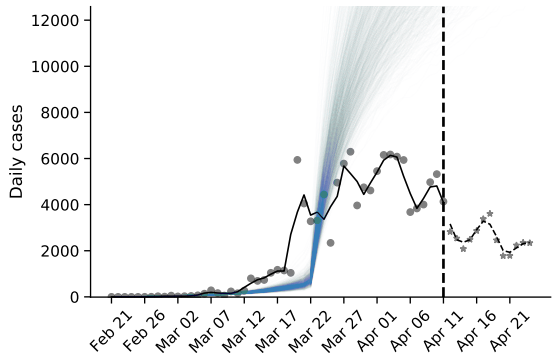
Denmark



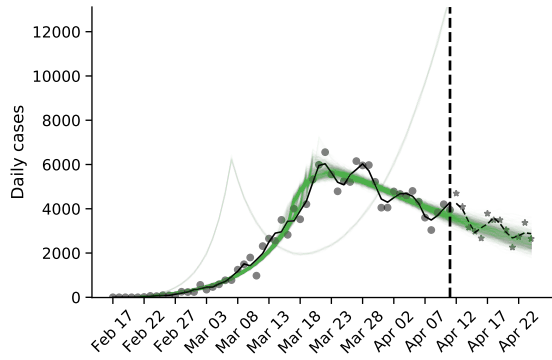
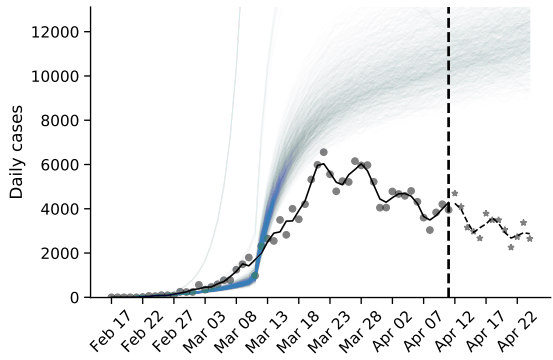
France



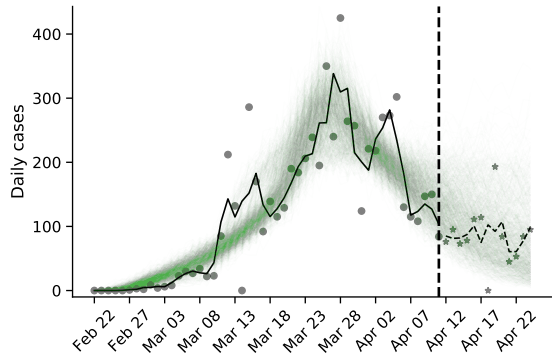
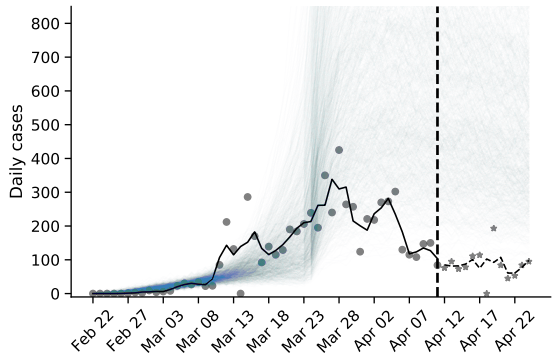
Germany



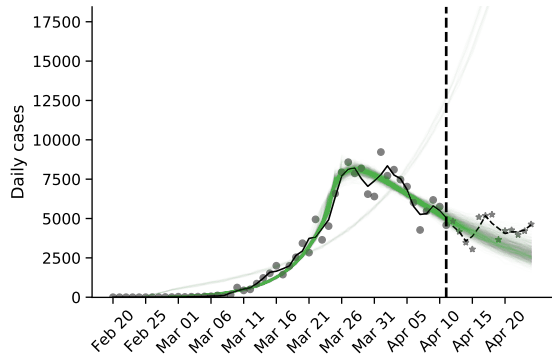
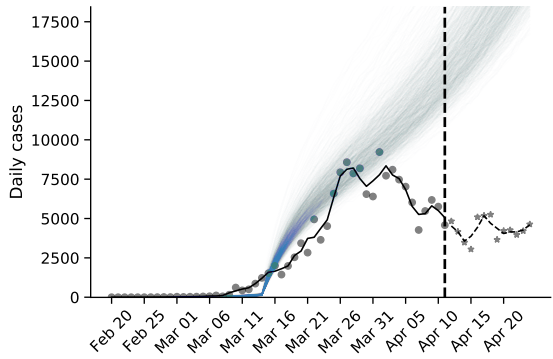
Italy



Norway



Spain



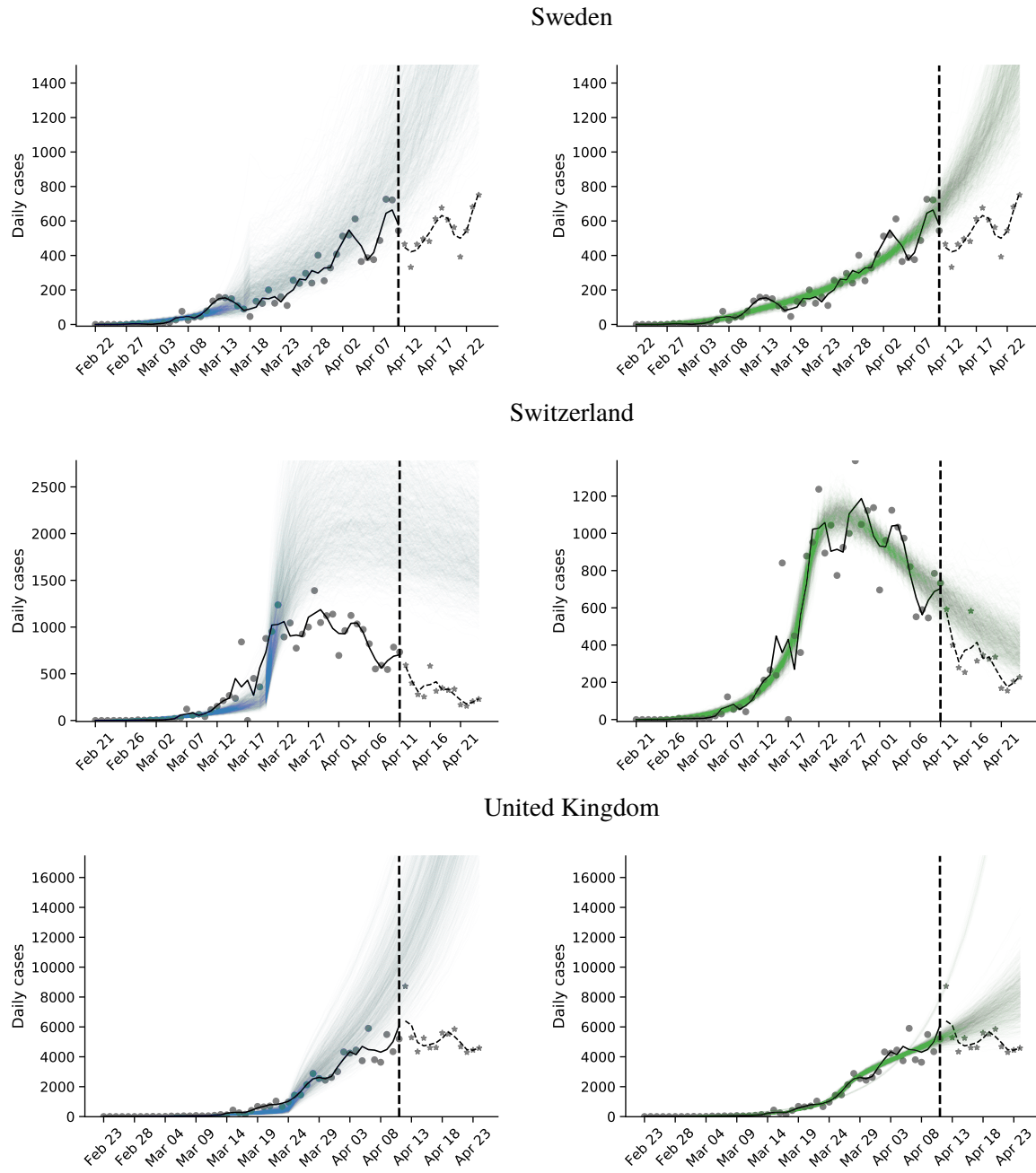


Figure S4. Posterior prediction plots for 11 European countries. Circles and stars represent daily case data up to and after Apr 11, 2020, respectively, and the vertical dashed line represents Apr 11. Black lines represents a smoothing of the data points using a Savitzky-Golay filter. Colored lines represent posterior predictions from a model with fixed τ – blue – and free τ – green. Models were fitted with data up to Apr 11. The predictions are generated by drawing 1,000 parameters sets from the posterior distribution, and then generating a daily case count using the SEIR model in Eq. 1. Note the differences in the y-axis scale. Posterior predictions with the free τ model are good for all countries except Denmark and Sweden, but poor for the fixed τ model. The predictions of the model without τ (not shown) are even worse.